

MULTIFOCUS IMAGE FUSION BASED ON MULTIREOLUTION AND MODIFIED PRINCIPAL COMPONENT ANALYSIS

C. Rama Mohan¹, S. Kiran², Vasudeva³ and A. Ashok Kumar⁴

¹Department of Computer Science and Engineering, Visvesvaraya Technological University, India

²Department of Computer Science and Engineering, YSR Engineering College of Yogi Vemana University, India

³Department of Computer Science and Engineering, Shri Madhwa Vadiraja Institute of Technology and Management, India

⁴Department of Physics, YSR Engineering College of Yogi Vemana University, India

Abstract

Multi-focus imaging fusion is a technique that puts together a fully focused object from the partly focused regions of several objects from the same scene. For producing a high quality fused image, negligible aliasing, and the ability to separate positive from negative frequencies characteristics are important. The ringed artifacts, however, were inserted into a fused image because of a lack of negligible aliasing and the ability to separate positive from negative frequencies properties. A multifocus image fusion algorithm is proposed to resolve these issues, in conjunction with multiresolution and modified principal component analysis. In this, two identical multi-focus images are considered, first they are subjected to the multi-resolution and then to the technique of modified principal component analysis. The multiresolution improves essential image features, which are best used in fusion of images, resulting in good image quality. Modified principal component analysis is applied to reduce the dimensionality of an image. The proposed fusion approach has been tested on a numeral of multifocus images and compared to various popular methods of imaging fusion. The experimental results indicate that in subjective performance and objective assessment, the proposed fusion approach could deliver better fusion results.

Keywords:

Multifocus Image Fusion, Multiresolution, Modified PCA, Evolution Metrics, Image Quality

1. INTRODUCTION

Multi-sensor data fusion has now become a technique that needs more general, systematic solutions for a variety of applications. Several situations in the processing of images in a single image involve high spatial and high spectral details. This is key in remote sensing. The instruments, however, are not able to provide this knowledge either by design or as a result of observational constraints. One logical solution is data fusion for this.

The mechanism of image fusion is specified to collect all important information from multiple images and incorporate it in fewer, typically a single image. This image, consisting of all content, is more insightful and accurate than any single source image. The fused method can not only reduce the data, but it can also generate pictures, which are more suitable and more understandable to human and machine perceptuality [1]. In computer view, multi-sensor image fusion is the method of merging appropriate information of two or several images to a single image [2]. The final image would be more accurate than any image [3].

Methods for image fusion can be commonly divided into two categories-spatial domain fusion and domain fusion transformation. Methods of fusion such as averaging, Brovey

method, principal component analysis (PCA) and IHS- methods come under approaches to space domains. Another essential form of spatial domain fusion is the technique that is based on high pass filtering. Here the specifics of the high frequency are inserted into upsampled version of MS images. Spatial domain approaches have the drawback that they create spatial distortion in the fused image. Spectral distortion is a detrimental factor when we go through more analysis, such as problem classification.

Analysis with multiresolution has become a very useful tool for analyzing remote sensing images. The discrete transformation of wavelets has become a very useful fusion tool. There are also several other forms of fusion, such as based on Laplacian pyramid, and curvelet transformation, etc. Such approaches show a higher performance of the fused image in spatial and spectral quality compared to other spatial fusion approaches.

The main intention to design different algorithms in image fusion is to reduce the redundant data and also to retain important information of the visual characteristics of the multi-source images. The images varying its spatial, temporal and spectral resolution characteristics may provide wide range information of the viewed objects [4]. Rapid innovative methodologies make it possible to produce fused images with high resolution containing spatial and spectral information [5]-[6]. The fusion of images has vast number of applications which includes medical imaging, police investigation, military, microscopical imaging, remote sensing, computer visual sense, and robotic visual sense and navigation.

Usually image fusion process is involved at one of the process stages such as pixel, signal and feature based levels. The well-known image fusion algorithms applied on the input images introduces serious effects such as decreasing the contrast of the image. At the later stages of the development, researchers are identified the importance to do the fusion process in the transform domain. With the evolution of wavelet theory, the multi-scale decomposition algorithmic rule is used in the image fusion process [7]. The analysis of images using wavelet domain found many applications image processing such as image restoration, removal of noise, enrichments of image edges and feature extraction. However, wavelet transforms are less efficient in acquiring information from two dimensional images [8].

Over the years many transform techniques have been recognized for the analysis of multi directional and multi-resolution images. However, the proposed techniques failed to provide good fused image in terms of obtaining reasonable values of the statistical parameters such as PSNR, Normalized correlation (NC) and MSE. Variety of transformation techniques are available in the literature among which wavelet transformation and cosine transformation are generally used in

image processing. In wavelet transformation algorithms, lifting wavelet and stationary wavelet transformation are majorly used. Discrete cosine transform (DCT) was frequently used by many researchers in group of cosine transforms.

Decomposition of multi-resolution images using variety of channels containing different frequency sub-bands in multi-scale. The decomposition operation applied on the image separates approximate and detailed component followed by 2-D DWT which converts the image from spatial domain to frequency domain. DWT operation not only gives spatial component such as frequency content of the input at different scales and also temporal component such as at what times these frequency components are presented. On the other hand, a DCT represented by a finite sequence of data points using the sum of cosine functions fluctuates at different frequencies. DCT algorithms are used in number of applications in engineering and science from lossy compression of audio and images to spectral methods to find the solution to partial differential applications.

Many algorithms were proposed with the combinations of DWT and PCA, Morphological processing and Combination of DWT with PCA and Morphological techniques [9] [12]. These methods show the best performance than simplex methods like averaging, minimum and maximum [13]. There is a lot of development in proposing pixel level based fusion algorithms. Majority of the fusion algorithms are based on wavelet transform [14]-[15], pyramid transform [16], statistical signal processing [17], principal component analysis [14] [17], fuzzy logic [18], DCT [13] [19] [20] and frequency portioning [21]. DCT technique gives better results for image compression and also accepted as more suitable and time saving technique for many image preprocessing applications [14].

This paper focuses on the fusion of multi-focus images using discrete cosine transformation with multiresolution and modified principal component analysis is applied to reduce dimensionality of an image. The feature extraction of the fused image is determined using various parametric analysis. The proposed method is also compared with already authorized fusion methods like LP, RP, DWT, DTCWT, CVT, NSCT, LP-SR, RP-SR, DWT-SR, DTCWT-SR, CVT-SR, NSCT-SR, MSVD, PC, SR, and MR. The result of MR-DCT with MPCA system shows that there is a much improvement in the statistical parameters than compared to other fusion methods.

2. NOISE ELIMINATION PROCESS

The size $P \times Q$ image $f(x,y)$ does separate toward rows and concatenates those rows into a 1D $f(x)$ array of data whose size will be PQ . This is explained in algorithm 1.

Algorithm 1: Conversion from 2D array to 1D array

Input: IR : 2D image, P : number of rows and Q : number of columns

Output: IR : 1D array data

Step 1. Start

Step 2. $IR(2:2:end,:) = IR(2:2:end,end:-1:1)$

Step 3. $IR = \text{reshape}(IR',1,P*Q)$

Step 4. Stop

The 2D image can be built from the data in the 1D array by reversing the procedure set out in algorithm 2.

Algorithm 2: Conversion from 1D array to 2D array

Input: IR : 1D array data, P : number of rows and Q : number of columns

Output: IR : 2D image

Step 1: Start

Step 2: $IR = \text{reshape}(IR,P,Q)'$

Step 3: $IR(2:2:end,:) = IR(2:2:end,end:-1:1)$

Step 4: Stop

Likewise, the size $P \times Q$ image $f(x,y)$ is divided into columns and concatenates those columns to form a 1D data $f(x)$ array whose size will be PQ as shown below. The operation is: $IR = \text{C2DT1D}(IR',P,Q)$. The fusion process is performed separately and combined on both row and column images to eliminate any noise or distortion created in the fusion process [22].

3. MULTIREOLUTION - DCT

The study of multiresolution [22] is discussed below. Data from the 1D array is transferred via DCT. Find the first half of the coefficients of DCT as LF and the rest as coefficients of HF. As shown below, the LF coefficients are passed through IDCT to obtain the vector data for the next decompositional step. Let $f_l(x) = f(x)$ at $l = 1$ level and at each l^{th} level:

$$f_l(u) = \text{DCT}(f_l(x)) \quad (1)$$

% low frequency components

$$X.L = \text{IDCT}(f_l(u)(1:0.5n)) \quad (2)$$

% high frequency frequency

$$X.H = f_l(u)(0.5n+1:n) \quad (3)$$

where subscript l shows the degree of decomposition of multi-resolution.

Let the images to fuse be $f_1(x,y)$ and $f_2(x,y)$ and the process of image fusion is as follows:

$$X_f.L = 0.5*(X_1\{J\}.L + X_2\{J\}.L) \quad (4)$$

$$D = (\text{abs}(X_1\{i\}.H) - \text{abs}(X_2\{i\}.H)) \geq 0 \quad (5)$$

$$X_f.H = D.*X_1\{i\}.H + (\sim D).*X_2\{i\}.H \quad (6)$$

The fused image can get using Eq.(4)-Eq.(6) by doing the procedure outlined in multiresolution.

4. MODIFIED PRINCIPAL COMPONENT ANALYSIS (M-PCA)

The M-PCA converts associated variables into several non-related main components, as a numerical method. This determines the optimal definition for a particular compact data set. The first principle of M-PCA is to estimate covariance values for a given set of data. The maximum variance is computed from the first principle component.

Let the source image is arranged as one column vector. The following steps are needed to project the data in 1D subspace.

Step 1: Arrange the data in a vector.

Step 2: Compute the covariance matrix for the given vector.

Step 3: Compute Eigenvalues for the given covariance matrix.

Step 4: Find out V, D from the Eigen function.

Step 5: Sort the D in order of decreasing eigenvalue.

Step 6: The first column computes V is the larger value of the Eigen. For estimating P as

$$P = V(:, \text{ind}(1)) ./ \text{sum}(V(:, \text{ind}(1))) \quad (7)$$

Step 7: Finally, to get the features extracted image as

$$PCA = P(1) * \text{Img} \quad (14)$$

To achieve the dimensionality reduction of an image, a novel MPCA method [23]-[25] is formulated, and the M-PCA method is explained in Algorithm 3 after image fusion is based on the MR.

Algorithm 3: M-PCA method

Input: Fused image by DTCWT.

Output: Features extracted image.

Step 1: Load the fused image.

Step 2: Compute $C = \text{cov}(\text{im1}(:))$

Step 3: $[V, D] = \text{eig}(C)$

Step 4: $[\text{max}, \text{ind}] = \text{sort}(\text{diag}(D), 'descend')$

Step 5: $a = V(:, \text{ind}(1)) ./ \text{sum}(V(:, \text{ind}(1)))$

Step 6: $F_E_img = a(1) * \text{im1}$

5. PROPOSED METHOD

The proposed system structure is shown in Fig.1, which involves two processes: the MRDCT-based image fusion process and the modified principal component analysis process. The two steps process model is shown in algorithm 4.

Algorithm 4: Image Fusion based on Multiresolution and M-PCA

Input: Images with multi-focus.

Output: All-in-Focus Image.

Step 1: Start

Step 2: Two multi-focus images (I_1 and I_2) are taken as source images to apply image fusion algorithm. Input images are divided into row (I_1 and I_2) and column (I_1 and I_2) pixels.

Step 3: Row and column pixels of multi focus images are converted from 2-D image into 1-D array data.

Step 4: The resultant 1-D array data (I_1) is decomposed into low (row and column frequencies) and high (row and column frequencies) frequency components using multiresolution. Similarly, the I_2 image is also decomposed into low (row and column frequencies) and high (row and column frequencies) frequency components.

Step 5: Primary fusion process is applied on row components (both low and high frequency components) of I_1 and I_2 to obtain low and high frequency row components. Similarly, the column components are also processed using this fusion process to obtain low and high frequency column components.

Step 6: Fused row and column frequency components are processed using Inverse Multi-resolute algorithm to obtain row and column components.

Step 7: Row and column components are converted from 1D array data into 2D image.

Step 8: From the processed row and column frequency components, final fused image is obtained using average fusion rule.

Step 9: Features extracted image is obtained after doing the M-PCA process on final fused image.

Step 10: Stop

6. RESULTS AND DISCUSION

The standard image test pairs (clock, lena, pepsi, hockey, and stadium) with multi focus were chosen by online resources such as www.imagefusion.org, www.mathworks.com, and www.github.com. These images were given as inputs for different standard fusion algorithms such as LP, RP, DWT, DTCWT, CVT, NSCT, LP-SR, RP-SR, DWT-SR, DTCWT-SR, CVT-SR, NSCT-SR, MSVD, PC, SR, and MR and Multiresolution + M-PCA (proposed method). The performance of these algorithms was analyzed using different visual and quantitative measures. The proposed algorithm fuse source images with multiresolution process and also Normalization is used to increase the dynamic range of the gray levels in the image.

Different statistical measures [26]-[30] such as RMSE, MAE, PSNR, SSIM, MSSIM, QM, and QTE used to quantify the performance of the fusion algorithms mentioned. The computed values of the statistical measures for different standard image test pairs using the mentioned fusion algorithms are specified in the table 1- 5. Based on the nature of these statistical measures, the values of PSNR, SSIM, MSSIM, QM and QTE should be of higher value and the other measures should be lower value to show the enhanced performance of the fusion algorithm. The images obtained after fusion process should be in such a way that it provides more necessary information based on people's perceptions, visual and quantitative analysis. The visual analysis of the fused image should reveal the significant improvement in the transfer of information from the source images, information lost from the source images and less artifacts.

The Fig.2 describes the standard clock images obtained by different image fusion algorithms. The image (Fig.2(t)) obtained from the proposed fusion algorithm shows better visual quality and less information loss. The statistical metrics evaluated for standard clock images using different fusion algorithms are specified in the Table.1. After the comparison of the statistical measures obtained by different fusion algorithms, the proposed method shows good performance over other standard fusion methods except QTE.

The standard lena images and images after various image fusion methods can be visualized in Fig.3. After the visual analysis of these images, the image obtained using the proposed method shows better quality and less information loss. The Table.2 shows the statistical measures of the different fusion algorithms and the metrics obtained for the proposed algorithm shows better values than compared to other algorithms.

Standard multifocus pepsi images obtained after applying to different fusion algorithms are shown in Fig.4. The pepsi image (Fig.4(t)) obtained using the proposed method shows the better visual appearance and appreciably more image quality. The Table.3 shows the quality metrics of the pepsi image using different fusion algorithms. From the visual appearance and quality metrics the proposed algorithm shows better performance than other algorithms.

The visual information of hockey images both input and output of various image fusion algorithms are shown in Fig.5. The Table.4 gives the statistical measures of the fusion algorithms of

the multifocus hockey image. After comparing the performance of the fusion methods, the proposed method shows good image quality and better statistical measures except QTE.

The Fig.6 shows the multifocus stadium images of various fusion algorithms. The fusion image obtained using proposed method shows better visual quality and appreciably no loss of information. The Table.5 gives the information about statistical measures of the stadium image processed with different image fusion algorithms. The comparison of the processed fusion images and statistical measures reveals that the proposed method shows better performance than other algorithms except QTE.

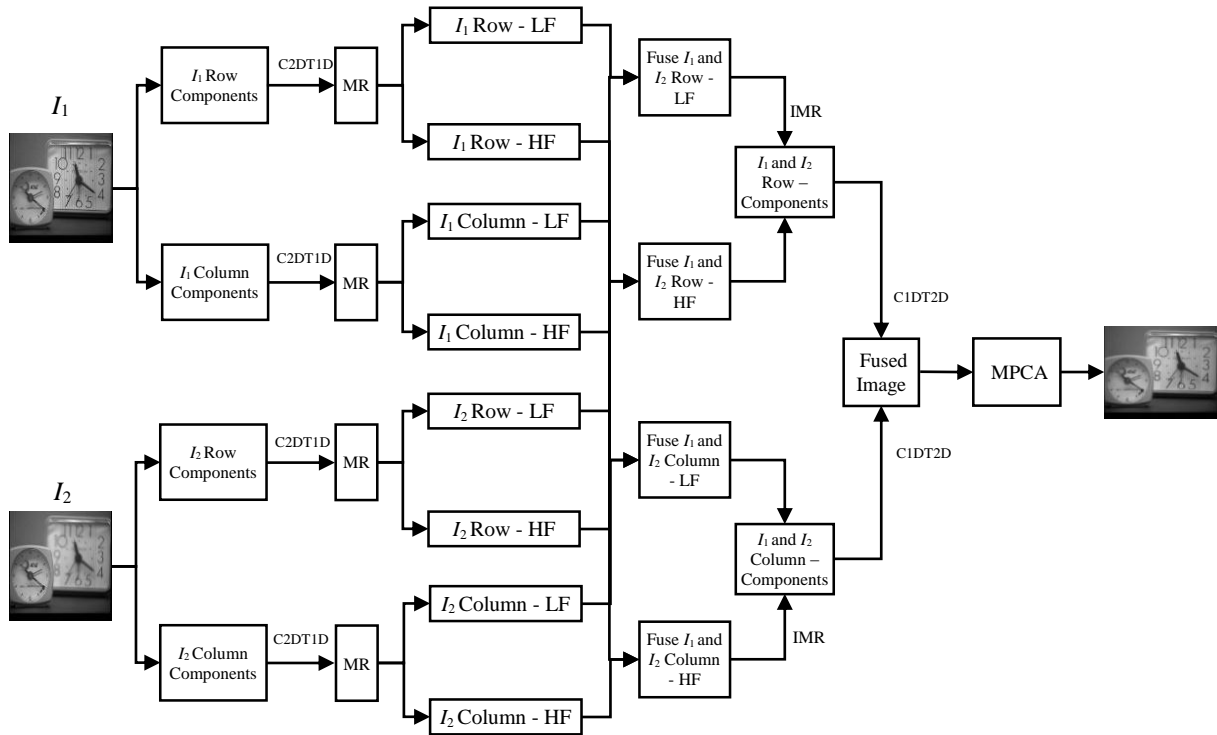


Fig.1. Flow diagram of proposed method

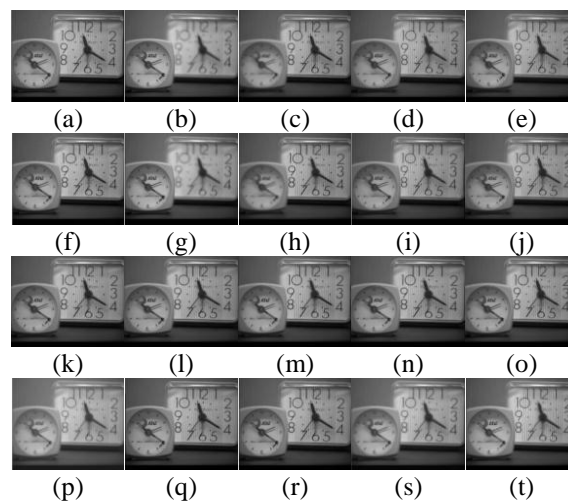


Fig.2. Multifocus Images (Clock): (a) Original Image (b) Input Image (X), (c) Input Image (Y), (d) LP, (e) RP, (f) DWT, (g) DTCWT, (h) CVT (i) NSCT (j) LP-SR (k) RP-SR (l) DWT-SR (m) DTCWT-SR (n) CVT-SR (o) NSCT-SR (p) MSVD (q) PC (r) SR (s) MR (t) Proposed Method

Table.1. Statistical measures of multifocus images (Clock) using different fusion algorithms

Algorithm	RMSE	MAE	PSNR	SSIM	MSSIM	QM	QTE
LP	4.040135512	2.482776204	42.10083998	0.993677079	0.993677079	1.157888442	0.43056011
RP	5.009549836	2.709151509	41.16681229	0.99234258	0.99234258	1.155105583	0.421872135
DWT	5.975676746	3.546512604	40.40092834	0.986999387	0.986999387	1.519805616	0.431632491
DTCWT	5.719931345	3.412534118	40.59089115	0.986245242	0.986245242	0.800535809	0.432140415
CVT	6.423948702	3.772151447	40.08677866	0.983338836	0.983338836	0.724413454	0.428745424
NSCT	2.748584176	1.670740254	43.77370889	0.99678155	0.99678155	1.958431017	0.427901314
LP_SR	3.514596958	1.920812446	42.70604402	0.99658984	0.99658984	1.738034338	0.438913511
RP_SR	3.329755136	1.876898038	42.94067633	0.996654704	0.996654704	2.14130445	0.430995725
DWT_SR	3.010944871	1.795351877	43.37777127	0.997568866	0.997568866	2.359313465	0.440944537
DTCWT_SR	2.786052629	1.674921041	43.71490615	0.997677747	0.997677747	2.101490018	0.438181725
CVT_SR	3.281743452	1.869497733	43.00375303	0.997591601	0.997591601	1.945454445	0.432736122
NSCT_SR	2.777325888	1.67482329	43.72853088	0.99706412	0.99706412	1.993130648	0.435466983
MSVD	8.6216652	4.988844501	38.80888776	0.974829953	0.974829953	0.471968327	0.42763848
PC	5.085914999	2.057052612	41.10110833	0.997295624	0.997295624	2.438973953	0.438951399
SR	3.244520101	1.86342271	43.05329462	0.996603864	0.996603864	2.07240923	0.431882739
Proposed Method	0.025851739	0.015620392	64.0399016	0.999973403	0.999996018	2.905707362	0.433740124

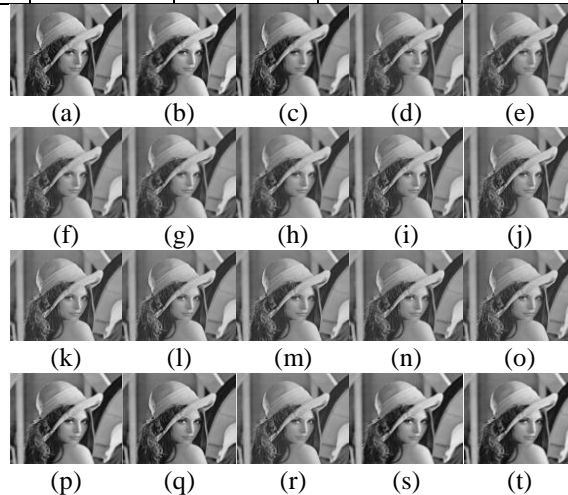


Fig.3. Multifocus Images (Lena): (a) Original Image (b) Input Image (X), (c) Input Image (Y), (d) LP, (e) RP, (f) DWT, (g) DTCWT, (h) CVT (i) NSCT (j) LP-SR (k) RP-SR (l) DWT-SR (m) DTCWT-SR (n) CVT-SR (o) NSCT-SR (p) MSVD (q) PC (r) SR (s) MR (t) Proposed Method

Table.2. Statistical measures of multifocus images (Lena) using different fusion algorithms

Algorithm	RMSE	MAE	PSNR	SSIM	MSSIM	QM	QTE
LP	3.376611227	1.828758488	42.8799887	0.99392641	0.99392641	0.870630052	0.413980834
RP	4.044798257	1.971692369	42.09583066	0.991923169	0.991923169	0.787372239	0.413160256
DWT	5.228118528	2.825413704	40.98134506	0.987096328	0.987096328	1.23380443	0.413054792
DTCWT	5.189588322	2.767607294	41.01347023	0.985702127	0.985702127	0.559779783	0.415906181
CVT	5.611565064	2.994773263	40.67395928	0.983303856	0.983303856	0.515121698	0.415165907
NSCT	1.280296466	0.750104815	47.09169384	0.998835107	0.998835107	1.764792678	0.416810684
LP_SR	1.446302215	0.453164388	46.56220879	0.999022136	0.999022136	1.677288136	0.420302451
RP_SR	1.582117706	0.269338521	46.1724114	0.999166838	0.999166838	2.098107907	0.427650145
DWT_SR	0.756077128	0.118642401	49.3791383	0.999730738	0.999730738	2.445426222	0.434385046
DTCWT_SR	0.557201034	0.067079054	50.70468017	0.999842842	0.999842842	2.351012701	0.436768616
CVT_SR	0.602017096	0.090616331	50.36871106	0.999813062	0.999813062	2.358795827	0.431484448
NSCT_SR	1.207634491	0.686667819	47.34544422	0.998916653	0.998916653	1.783700891	0.416013549

MSVD	5.904515378	3.370568812	40.45295673	0.982295963	0.982295963	0.515487282	0.418382277
PC	0.822907911	0.05116272	49.01128693	0.999593195	0.999593195	2.462695013	0.445754312
SR	0.461720269	0.031191182	51.52100991	0.99987477	0.99987477	2.445900051	0.441394712
Proposed Method	0.022938972	0.012930373	64.55905979	0.999969967	0.999995881	2.895197566	0.450381789

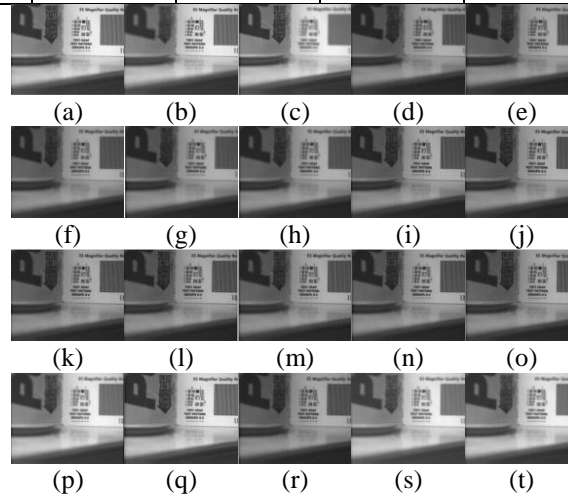
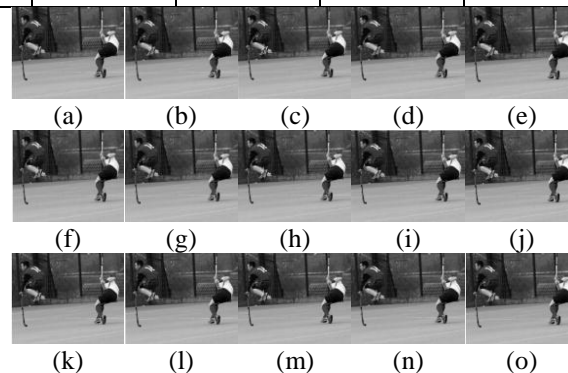


Fig.4. Multifocus Images (Pepsi): (a) Original Image (b) Input Image (X), (c) Input Image (Y), (d) LP, (e) RP, (f) DWT, (g) DTCWT, (h) CVT (i) NSCT (j) LP-SR (k) RP-SR (l) DWT-SR (m) DTCWT-SR (n) CVT-SR (o) NSCT-SR (p) MSVD (q) PC (r) SR (s) MR (t) Proposed Method

Table.3. Statistical measures of multifocus images (Pepsi) using different fusion algorithms

Algorithm	RMSE	MAE	PSNR	SSIM	MSSIM	QM	QTE
LP	3.394757308	1.869426938	42.85671199	0.99096639	0.99096639	1.377042335	0.439282128
RP	3.784052373	1.965768303	42.38522792	0.988352009	0.988352009	1.260219002	0.434663491
DWT	5.208042559	2.684242249	40.99805406	0.98388609	0.98388609	1.548450446	0.440732943
DTCWT	5.111583838	2.570903428	41.07924442	0.982539251	0.982539251	1.12418495	0.443727215
CVT	5.685989894	2.789473574	40.61673847	0.979008839	0.979008839	1.040653043	0.446532929
NSCT	1.690562441	1.057270897	45.88448715	0.996385571	0.996385571	1.728545838	0.455205724
LP_SR	1.483228073	0.935957428	46.45271994	0.996520143	0.996520143	1.632615148	0.445599846
RP_SR	1.834257671	0.961724577	45.53019587	0.996183699	0.996183699	1.978649248	0.441795787
DWT_SR	1.474847108	0.935159509	46.4773293	0.996741773	0.996741773	2.254490318	0.445054489
DTCWT_SR	1.546095745	0.908732812	46.27243546	0.996524733	0.996524733	1.819531389	0.438620884
CVT_SR	1.420883862	0.88028884	46.63921349	0.996540223	0.996540223	1.675036596	0.448168212
NSCT_SR	1.689312147	1.077252626	45.88770026	0.996088636	0.996088636	1.746609973	0.459370882
MSVD	8.450150922	3.957128299	38.89615465	0.970969741	0.970969741	0.704906694	0.42390182
PC	1.832290468	1.075313568	45.53485608	0.99426248	0.99426248	2.315735686	0.449905527
SR	3.688755474	1.71433445	42.49600064	0.988705676	0.988705676	1.130443629	0.432071544
Proposed Method	0.022503365	0.011032538	64.64232469	0.999970101	0.999996133	2.926523922	0.476047333



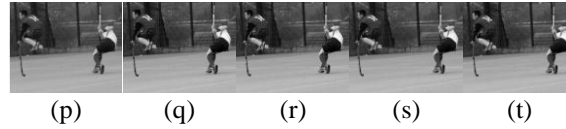


Fig.5. Multifocus Images (Hockey): (a) Original Image (b) Input Image (X), (c) Input Image (Y), (d) LP, (e) RP, (f) DWT, (g) DTCWT, (h) CVT (i) NSCT (j) LP-SR (k) RP-SR (l) DWT-SR (m) DTCWT-SR (n) CVT-SR (o) NSCT-SR (p) MSVD (q) PC (r) SR (s) MR (t) Proposed Method

Table.4. Statistical measures of multifocus images (Hockey) using different fusion algorithms

Algorithm	RMSE	MAE	PSNR	SSIM	MSSIM	QM	QTE
LP	3.860400907	0.75291463	42.29847522	0.999699229	0.999699229	1.195912135	0.424173776
RP	3.856462567	0.727426011	42.3029081	0.999675396	0.999675396	1.136500222	0.42357762
DWT	4.256881869	1.692272368	41.87388332	0.997658002	0.997658002	1.241178441	0.415841531
DTCWT	3.305494461	1.282886851	42.97243497	0.998585683	0.998585683	0.613326167	0.42209435
CVT	3.302606179	1.505441626	42.97623142	0.9979018	0.9979018	0.5628002	0.414214294
NSCT	3.930251759	0.573815796	42.2205956	0.999822591	0.999822591	2.059551314	0.425657944
LP_SR	4.095119455	0.86569065	42.04213356	0.998942871	0.998942871	1.22241373	0.426684131
RP_SR	3.730157759	0.39513246	42.44752731	0.999593361	0.999893361	2.143033439	0.42675629
DWT_SR	3.208574355	0.477567076	43.10167823	0.999547038	0.999847038	2.227417103	0.432499478
DTCWT_SR	3.817464939	0.363924273	42.34704874	0.9990295	0.99990295	2.158725457	0.428881759
CVT_SR	2.375421332	0.394064929	44.40739278	0.999842442	0.999842442	2.119438012	0.422308052
NSCT_SR	4.127784332	0.498999238	42.00762932	0.99987722	0.99987722	2.064092054	0.428928696
MSVD	12.50686951	6.079739815	37.19331312	0.972172428	0.972172428	0.22049222	0.378813047
PC	1.120436034	0.152765765	47.67092863	0.999417035	0.999417035	2.181453407	0.430481871
SR	3.079476772	0.223903379	43.28002998	0.99928899	0.999928899	2.212044777	0.42992256
Proposed Method	0.016530977	0.009409421	65.98181415	0.999995808	0.999999338	2.887379318	0.414799302

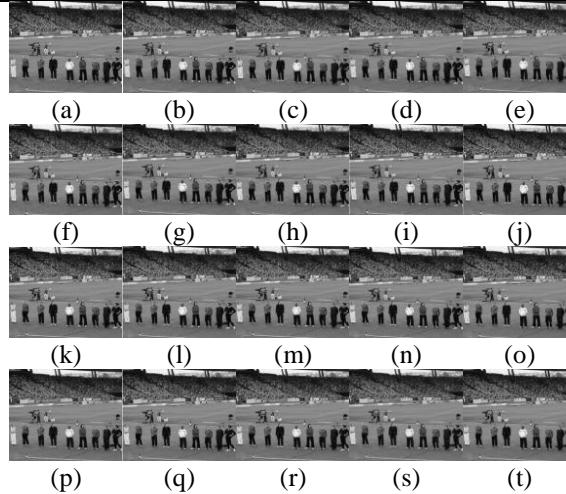


Fig.6. Multifocus Images (Stadium): (a) Original Image (b) Input Image (X), (c) Input Image (Y), (d) LP, (e) RP, (f) DWT, (g) DTCWT, (h) CVT (i) NSCT (j) LP-SR (k) RP-SR (l) DWT-SR (m) DTCWT-SR (n) CVT-SR (o) NSCT-SR (p) MSVD (q) PC (r) SR (s) MR (t) Proposed Method

Table.5. Statistical measures of multifocus images (Stadium) using different fusion algorithms

Algorithm	RMSE	MAE	PSNR	SSIM	MSSIM	QM	QTE
LP	3.223940783	1.017870381	43.08092875	0.999604065	0.999604065	1.121705935	0.356804376
RP	3.189647052	0.992540269	43.12737301	0.999527546	0.999527546	1.003414877	0.359164376
DWT	6.293364712	3.533436055	40.1759703	0.995429844	0.995429844	1.099425075	0.344795185
DTCWT	4.364783134	2.454274518	41.7651726	0.997724794	0.997724794	0.464416318	0.346050799
CVT	4.838205595	2.957511992	41.31795611	0.996424134	0.996424134	0.425316817	0.34125213

NSCT	2.838353507	0.453144612	43.63413446	0.9993967	0.9998967	2.196968139	0.369247798
LP_SR	5.213062894	1.589705391	40.99386966	0.997392165	0.997392165	1.046351428	0.368709442
RP_SR	2.808939855	0.303716554	43.6793749	0.999893205	0.999893205	2.291295648	0.381813813
DWT_SR	3.214674327	0.50626775	43.09342949	0.999729194	0.999729194	2.373782048	0.388455254
DTCWT_SR	2.042391212	0.208965724	45.06340998	0.99922875	0.999922875	2.32416969	0.387928376
CVT_SR	2.147116074	0.362315461	44.84624408	0.999875754	0.999875754	2.218026811	0.365890113
NSCT_SR	2.907240308	0.425461162	43.52998999	0.99908587	0.999908587	2.201249853	0.375278766
MSVD	12.9425817	7.66408798	37.04459015	0.9873047	0.9873047	0.167868193	0.345118121
PC	4.003209909	0.4453125	42.14071568	0.998961179	0.998961179	2.3547238	0.371618407
SR	1.646613927	0.107817035	45.99888146	0.99916894	0.999916894	2.336919456	0.371415334
Proposed Method	0.03451698	0.023792056	62.78447145	0.999978319	0.999997112	2.841773035	0.327522594

The results illustrate that not only the proposed fusion algorithm applied to all five multifocus image sets shows better visual performance but also the statistical measures proved the same than compared to other fusion methods. It is also evidenced that the proposed algorithm shows better visual appearance and also exhibits better statistical measures than compared to other methods published recently [24] [31]-[32].

7. CONCLUSION

It was proposed and applied to image fusion Multiresolution (MR) using M-PCA technique. A variety of other methods were developed using and compared LP, RP, DWT, DTCWT, CVT, NSCT, LP-SR, RP-SR, DWT-SR, DTCWT-SR, CVT-SR, NSCT-SR, MSVD, PC, SR, and MR. Various quality control methods are tested to check the reliability of images. The proposed MR with M-PCA shows better measurement efficiency, which in effect improves image quality without losing information or without losing artifacts, among different techniques used on various pairs of multifocus images.

REFERENCES

- [1] M. Amin-Naji and A. Aghagolzadeh, "Multi-Focus Image Fusion in DCT Domain using Variance and Energy of Laplacian and Correlation Coefficient for Visual Sensor Networks", *Journal of AI and Data Mining*, Vol. 6, No. 2, pp. 233-250, 2018.
- [2] M.B.A. Haghghat, A. Aghagolzadeh and H. Seyedarabi, "Multi-Focus Image Fusion for Visual Sensor Networks in DCT Domain", *Computers and Electrical Engineering*, Vol. 37, No. 5, pp. 789-797, 2011.
- [3] M.B.A. Haghghat, A. Aghagolzadeh and H. Seyedarabi, "A Non-Reference Image Fusion Metric based on Mutual Information of Image Features", *Computers and Electrical Engineering*, Vol 37, No. 5, pp. 744-756, 2011.
- [4] C. Pohl and J.L. Van Genderen, "Multisensor Image Fusion in Remote Sensing: Concepts, Methods, and Applications", *International Journal on Remote Sensing*, Vol. 19, No. 5, pp. 823-854, 1998.
- [5] Susmitha Vekkot and Pancham Shukla, "A Novel Architecture for Wavelet based Image Fusion", *World Academy of Science, Engineering and Technology*, Vol. 57, pp. 372-377, 2009.
- [6] Gonzalo Pajares and Jesus Manuel De La Cruz, "A Wavelet-Based Fusion Tutorial", *Pattern Recognition*, Vol. 37, pp. 1855-1872, 2004.
- [7] Heng Ma, Chuanying Jia and Shuang Liu, "Multisource Image Fusion Based on Wavelet Transform", *International Journal on Information Technology*, Vol. 11, No. 7, pp. 81-91, 2005.
- [8] Mark J. Shensa, "The Discrete Wavelet Transform: Wedding the Trous and Mallat Algorithms", *IEEE Transactions on Signal Processing*, Vol. 40, No. 10, pp. 2464-2482, 1992.
- [9] Yufeng Zheng, Edward A. Essock and Bruce C. Hansen, "An Advanced Image Fusion Algorithm based on Wavelet Transform: Incorporation with PCA and Morphological Processing", *Proceedings of International Conference on Electronic Imaging*, pp. 177-187, 2004.
- [10] Shrivsubramani Krishnamoorthy and K. P. Soman, "Implementation and Comparative Study of Image Fusion Algorithms", *International Journal on Computer Applications*, Vol. 9, No. 2, pp. 231-245, 2010.
- [11] W. Svante, "Principal Component Analysis Chemometrics and Intelligent Laboratory Systems", Elsevier Science Publisher, 1987.
- [12] C. Rama Mohan, S. Kiran and R. Pradeep Kumar Reddy, "Multi-Focus Image Synthesis based on DWT and Texture with Sharpening", *Pezzottaite Journals*, Vol. 4, No. 4, pp. 1662-1670, 2015.
- [13] C. Rama Mohan, S. Kiran and R. Pradeep Kumar Reddy, "A Study on Several Image Synthesis Algorithms", *Pezzottaite Journals*, Vol. 4, No. 3, pp. 1600-1608, 2015.
- [14] V.P.S. Naidu and J.R. Raol, "Fusion of Out of Focus Images using Principal Component Analysis and Spatial Frequency", *Journal on Aerospace Sciences and Technologies*, Vol. 60, No. 3, pp. 216-225, 2008.
- [15] H. Li, B.S. Manjunath and S.K. Mitra, "Multisensor Image Fusion using the Wavelet Transform", *Graphical Models and Image Processing*, Vol. 57, No. 3, pp. 235-245, 1995.
- [16] A. Toet, "Image Fusion by a Ratio of Low-Pass Pyramid", *Pattern Recognition Letters*, Vol. 9, No. 4, pp. 245-253, 1989.
- [17] V.P.S. Naidu and J.R. Raol, "Pixel-Level Image Fusion using Wavelets and Principal Component Analysis-A Comparative Analysis", *Defence Science Journal*, Vol. 58, No. 3, pp. 338-352, 2008.
- [18] Amaj Chamankar, Mansour Sheikhan and Farhad Razaghian, "Multi-Focus Image Fusion using Fuzzy Logic",

- Proceedings of Iranian Conference on Fuzzy Systems*, pp. 25-29, 2013.
- [19] V.P.S. Naidu, "Discrete Cosine Transform based Image Fusion Techniques", *Communication, Navigation and Signal Processing*, Vol. 1, No. 1, pp. 35-45, 2012.
- [20] V.P.S. Naidu, "Block DCT based Image Fusion Techniques", *e-Journal of Science and Technology*, Vol. 2, No. 1, pp. 49-66, 2013.
- [21] Veerpal Kaur and Jaspreet Kaur, "Frequency Partitioning Based Image Fusion for CCTV", *International Journal on Computer Science and Information Technologies*, Vol. 6, No. 4, pp. 3968-3972, 2015.
- [22] V.P.S. Naidu, "Novel Image Fusion Techniques using DCT", *Computer Science and Business Informatics*, Vol. 5, No. 1, pp. 45-56, 2013.
- [23] C. Rama Mohan, S. Kiran, Vasudeva and A. Ashok Kumar, "Image Enhancement based on Fusion using 2D LPDCT and Modified PCA", *International Journal of Engineering and Advanced Technology*, Vol. 8, No. 3, pp. 1482-1492, 2019.
- [24] C. Rama Mohan, S. Kiran and A. Ashok Kumar, "Advanced Multifocus Image Fusion algorithm using FPDCT with Modified PCA", *International Journal of Innovative Technology and Exploring Engineering*, Vol. 9, No. 2, pp. 175-184, 2019.
- [25] C. Rama Mohan, S. Kiran, Vasudeva and A. Ashok Kumar, "Multi-Focus Image Fusion Method with Qshift N-DTCWT and Modified PCA in Frequency Partition Domain", *ICTACT Journal on Image and Video Processing*, Vol. 11, No. 1, pp. 2275-2282, 2020.
- [26] C.R. Mohan and S. Kiran, "Image Enrichment Using Single Discrete Wavelet Transform Multi-resolution and Frequency Partition", *Proceedings of International Conference on Artificial Intelligence and Evolutionary Computations in Engineering Systems*, pp. 542-561, 2018.
- [27] P. Jagalingam and A.V. Hegde, "A Review of Quality Metrics for Fused Image", *Aquatic Procedia*, Vol. 4, No. 2, pp. 133-142, 2015.
- [28] Betsy Samuel and N. Vidya, "Full Reference Image Quality Assessment for Biometric Detection", *International Journal on Modern Trends in Engineering and Research*, Vol. 2, No. 6, pp. 1-13, 2015.
- [29] Mayuresh Gulame, K.R. Joshi and Kamthe, "A Full Reference Based Objective Image Quality Assessment", *International Journal on Advanced Electrical and Electronics Engineering*, Vol. 2, No. 6, pp. 123-129, 2013.
- [30] Ratchakit Sakuldee and Somkait Udomhunsakul, "Objective Performance of Compressed Image Quality Assessments", *International Journal on Computer and Information Engineering*, Vol. 4, No. 1, pp. 34-45, 2007.
- [31] Pedram Mohammadi, Abbas Ebrahimi-Moghadam and Shahram Shirani, "Subjective and Objective Quality Assessment of Image: A Survey", *Signal Processing Image Communication*, Vol. 85, pp. 1-24, 2014.
- [32] C. Rama Mohan, S. Kiran, Vasudeva and A. Ashok Kumar, "Image Enhancement based on Fusion using 2D LPDCT and Modified PCA", *International Journal of Engineering and Advanced Technology*, 8(6S3), pp. 1-8, 2019.
- [33] C. Rama Mohan, S. Kiran, Vasudeva and A. Ashok Kumar, "An Efficient Multifocus Image Fusion method using Curvelet Transform and Normalization", *International Journal of Future Generation Communication and Networking*, Vol. 13, No. 3, pp. 2946-2958, 2020.